LOADABILITY LIMITS AND EMERGENCY COUNTERMEASURES AGAINST VOLTAGE COLLAPSE

M. E. Karystianos V. C. Nikolaidis C. D. Vournas
National Technical University of Athens
School of Electrical & Computer Engineering
Athens, Greece
vournas@power.ece.ntua.gr

Abstract – This paper proposes a method for loadability limit computation using a uniform load increase. The normal vector to the loadability surface at this point is used to identify the region affected by the loadability. Following this a two-dimensional load space is defined on which the loadability surface is plotted. Loadability margin sensitivity is used to design a load-shedding scheme to achieve a required margin. A heavily stressed snapshot of the Hellenic system is used to test the above methods.

Keywords: Voltage stability, Voltage security, Loadability limits, Emergency control, Load Shedding

1 INTRODUCTION

Loadability limits are critical points of particular interest in voltage stability assessment, indicating how much a system can be stressed from a given state before reaching instability [1]. In recent years, the restructuring of power systems and the application of open access principles in energy markets, led power systems to operate under higher stress conditions, and therefore closer to loadability limits. Recent blackouts in many countries are indicative of this trend.

This paper presents a method to compute loadability limits based on a uniform direction of load increase and generation adjustment. Under certain conditions, this limit will give the smallest percentage of load increase to reach loadability [2]. The information provided by the vector normal to the bounding branch of the loadability surface at the computed loadability limit is used to separate the system in two basic regions: the one mostly affected by the instability and the area relatively unaffected. Based on this separation the loadability surface is visualized in two dimensions corresponding to the total load consumed in each of the above two regions. A proportional load variation within each of these regions is assumed.

The loadability limits can correspond to a particular operating point without any contingency, or they can be computed for a specific disturbance, in which case they are called post-contingency loadability limits [3]. The method presented in this paper can be used for on-line (real-time), as well as off-line security assessment. For simplicity of presentation an on-line environment will be assumed, for which the critical contingency has already been selected.

The distance (percentage of load increase) between the current operating point and the closest loadability limit defines the loadability margin. When the loadability margin is less than acceptable, preventive and corrective actions have to be taken. In particular, if the loadability margin is less than the expected load increase during the day, the system is in an emergency state and even extreme countermeasures, such as load shedding [4] have to be taken to avoid a blackout.

In this paper we consider a load-shedding scheme that is based on the information provided by the sensitivity of loadability margin [5]. A fixed percentage of load reduction at each load bus is assumed. Buses for load shedding are selected starting from the bus with the largest margin sensitivity until the desired loadability margin (based on sensitivity information) is achieved.

The above methodology is applied to an extremely stressed operating point of the Hellenic Interconnected System, just prior to the Athens blackout that occurred on July 12, 2004. This is taken as a typical case of a stressed power system to quantify the results of this paper, which is by no means attempting an analysis of the events of that day.

This paper is organized as follows. Section 2 summarizes the properties of loadability surface and some relative concepts. In Section 3 we present an algorithm for loadability limit computation and loadability surface visualization. In Section 4 the above techniques are applied to a heavily stressed operating point of the Hellenic Interconnected System. Section 5 describes some features of the quasi steady state simulation program WPSTAB [3] used to validate the proposed load shedding scheme. In particular the way in which armature current limitation is included in the simulation is described. In Section 6 the information from the loadability limit computation tool is used to apply load shedding to a heavily stressed operating point of the system. Finally section 7 summarizes the basic results from the analysis presented.

2 LOADABILITY LIMITS

2.1 Loadability Margin

Loadability limits can be defined as the points where the load demand reaches a maximum value, after which no viable operating points of the system exist. If the load is considered as constant power, the loadability limit equals to the maximum deliverable power to a system bus, or number of buses.

Loadability limits can be computed either on the current configuration of a power system, in order to assess the system ability to face a forecasted load increase, or for the operating point after the appearance of a disturbance. In the latter case we refer to post-contingency loadability limits, which are useful for characterizing the security level of a power system.

In association to a loadability limit, a loadability margin can be determined. This margin expresses the distance from the operating point to the loadability limit using some norm. Whenever the operators of the system consider the loadability margin insufficient, preventive countermeasures have to be taken in order to restore power system security.

A critical factor affecting loadability limits and associated margins is the direction of system stress. By system stress we mean a change in load and generation, according to a specific pattern. Stress direction indicates the participation of active and reactive loads and active generation to the overall power change.

2.2 Loadability Surface & Types of Loadability Limits

Generally the set of loadability limits in load parameter space forms a boundary of the solution space of equilibrium equations of a power system that is known as loadability surface. The loadability surface is possible to display quite complicated behaviour [6] and consists, in the general case, of multiple intersecting smooth branches [7]. In this way various loadability limits with different attributes can be identified on a loadability surface. Specifically:

- *Saddle-node bifurcations* (SNB), where the limit is due to smooth dynamics and the state Jacobian of equilibrium equations becomes singular.
- *Switching loadability limits*, that are due to an immediate change in stability, after a discrete event e.g. when a generator reaches its reactive power limit [8].
- *Corner points*, that are due to several switching actions occurring simultaneous (e.g. generators reach excitation limit simultaneously) [2].

2.3 Normal Vector

At a loadability limit, the Jacobian of system dynamics can be singular having a zero eigenvalue or nonsingular having an eigenvalue changing sign abruptly due to switching actions. In the first case the loadability limit corresponds to a bifurcation point, whereas in the latter case the loadability limit corresponds to a switching point. In any case, at a simple loadability limit that is not a corner point, the left eigenvector or singular vector $\mathbf{w}$ can be determined [2], providing the necessary information for the calculation of the normal vector $\mathbf{n}$ to the loadability surface:

$$\mathbf{n} = D_{\mathbf{p}} \boldsymbol{\psi}^T \cdot \mathbf{w} \tag{1}$$

where $\boldsymbol{\psi}$ denotes the vector of equilibrium equations including (for switching loadability limits) the active constrains that hold as equalities at the loadability limit [1,2,7]. In the case of a corner point due to several switching conditions, for each switching condition we have a separate set of equations $\boldsymbol{\psi}_\mathbf{i}$ that define a singular vector $\mathbf{w_i}$, and thus from (1) a different vector $\mathbf{n_i}$, which is normal to the relative loadability branch [2].

The normal vector can be used to provide the direction for the countermeasures against voltage instability, such as load shedding [4]. In Fig. 1 the loadability surface in a two-dimensional load parameter space and the direction of the normal vector at a point C are shown. As seen, the normal vector indicates the optimum direction (in a Euclidian sense) to move away from the loadability surface.

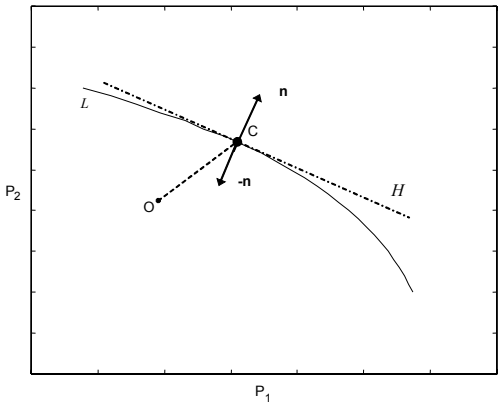

Figure 1: Normal vector to loadability surface

2.4 Minimum percentage of loadability margin

Another important problem for power system security is that of determining the closest loadability limit to an operating point O, and therefore the minimum loadability margin. The minimum load power margin is a useful index of proximity to voltage collapse.

In [9] iterative and direct methods are proposed to compute the closest saddle-node bifurcation to an operating point using the L_2-norm (Euclidian distance). Other approaches, such as in [4], consider the sum of loads described by the L_1-norm. To avoid load directions that are unrealistic (either for increasing load, or recovering from a loadability limit), limits can be set to individual load variations.

In [2] we have proposed a normalization of load parameters:

$$\lambda_i = \frac{p_i - p_{io}}{p_{io}} \tag{2}$$

so that λ_i is the percentage of load increase for bus i. Assuming that normal vector elements are always positive:

$$n_i > 0 \tag{3}$$

it is easily shown [2] that the uniform direction of stress provides the minimum loadability margin (in percentage of any load). Note that in this way the distance to loadability is measured using the L_∞ norm in the normalized load power space. The geometrical representation of the

closest loadability limit in this sense is that of inscribing the largest possible square in the feasibility region, as shown in Fig. 2. For any percentage of load increase not exceeding the calculated margin, the system is secure.

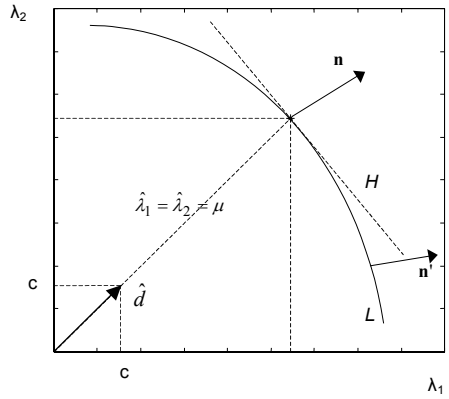

Figure 2: Closest loadability limit for L_∞ norm

Note that assumption (3) requires all loads to contribute to the loadability, i.e. for a point on the loadability surface any load reduction will restore a feasible operating point. This is a typical condition for voltage stability constrained systems.

By applying a uniform load increase all loads are varied by the same percentage λ:

$$P_i = P_{io}(1+\lambda) \tag{4a}$$

$$Q_i = Q_{io}(1+\lambda) \tag{4b}$$

where P_{io} and Q_{io} are the base case active and reactive loads. The maximum value of λ corresponding to the loadability limit is denoted by μ and corresponds to the loadability margin in percent. This margin can be easily translated to MW, which is much more meaningful to system operators, simply multiplying by the total active load at the base case:

$$M = \mu \sum P_{io} = \mu P_o \tag{5}$$

where M is the loadability margin in MW.

2.5 Sensitivities of loadability margin

Sensitivities of loadability margin to load power are calculated straightforward based on the work originally presented in [5]. The sensitivity formula as given in [1] is:

$$\mathbf{S}_\mu = -\frac{\mathbf{n}}{\mathbf{n}^T \mathbf{d}} \tag{6}$$

where $\mathbf{S}_\mu$ is the vector of sensitivities of the loadability margin with respect to the load parameters, **n** is the normal vector to the loadability surface, and **d** is the direction of stress, which for the uniform stress is equal to the base case load $\mathbf{p_o}$. At each load bus a single sensitivity $S_{\mu Pi}$ is computed combining the elements of $\mathbf{S}_\mu$ corresponding to the active and reactive load, thus assuming a constant power factor.

Clearly the largest bus sensitivities indicate the load buses, which have the strongest influence on the loadability margin. The bus sensitivities can also be expressed in MW of load margin by multiplying by P_o. In this case, a sensitivity value larger than one means that for each MW shed a larger increase in margin is achieved as the other loads can be further stressed.

3 LOADABILITY LIMIT COMPUTATION

3.1 QSS simulation

Quasi-Steady-State (QSS) simulation [1,3] is a very powerful tool for voltage security analysis. In this section we explain how a modified QSS simulation tool can be used to obtain the loadability margin.

As explained before we are content to explore a uniform direction of load increase. Thus, in the simulation a smooth load demand ramp is imposed on all system loads, which are assumed voltage sensitive. System controllers and protection devices, such as Load Tap Changers (LTCs), generator overexcitation limiters etc., are explicitly modelled.

The increase in load demand results in a voltage decline causing the activation of the LTCs, which tend to restore secondary voltage in distribution buses and subsequently the power consumed by the corresponding loads. However, due to LTC deadbands, the system trajectory may diverge from the specified direction of stress. This effect becomes more pronounced as LTCs hit their hard tap limits. In order to overcome the above handicaps we propose in the next subsection a modified simulation method that takes account a full load restoration process. We will return to normal QSS simulation in Section 5.

3.2 A Simulation Method for Loadability Computation

The modified QSS simulation serves two purposes. First, it takes into account the evolution of the system thus representing the potentially complex series of time dependent events, which influence loadability. On the other hand, in order to maintain the direction of stress, additional equations are introduced to force constant power restoration. For a voltage sensitive load with active and reactive load exponents *a* and *b* respectively the following equality constraints for each bus are added:

$$\left(\frac{P_{di}}{V_{oi}^a}\right) V_i^a - P_{oi}(1+\lambda) = 0 \tag{7a}$$

$$\left(\frac{Q_{di}}{V_{oi}^b}\right) V_i^b - Q_{oi}(1+\lambda) = 0 \tag{7b}$$

where V_{oi} and V_i are the initial and current bus voltages and P_{di}, Q_{di} are the active and reactive load demands respectively. An augmented Jacobian including (7) is formed.

The percentage of load increase at the end of simulation run is the desired loadability margin μ. In order to prevent excessive variations of load demand, at every step of the simulation LTCs are adjusted first, so as to restore load voltage within its deadband, thus restoring also load power to a certain extent. In that sense (7) is

used to provide initially the fine tuning necessary to maintain the uniform load increase, but inevitably the load demand is progressively increased as simulation evolves and system comes closer to loadability limit. Since the unlimited load demand increase is by nature a pessimistic assumption, this is partly compensated by allowing also an unlimited voltage regulation ignoring the lower tap limits of HV/MV tap changers.

The loadability limit can be found either by the loss of equilibrium due to an SNB, or an "oscillation" between operation modes of switching devices of one or more generators (such as Automatic Voltage Regulator & Overexcitation Limiter) at the same load level, in case of a switching loadability limit, or a corner point. In the latter cases, during the switching a long-term sensitivity index changes sign [1]. In all cases the nature of the loadability limit is checked, so as to avoid cases of purely numerical divergence. This is achieved by relaxing the constraints (7) to find the nearest point lying exactly on the loadability surface. The normal vector of the loadability surface at this point is compared to that computed at the last converged solution on the uniform stress direction, and if the two are close enough, the latter point is considered a loadability limit.

Once the loadability limit is sufficiently approximated, the sensitivities of the margin with respect to bus loads are computed, providing the necessary information for possible countermeasures.

3.3 Affected area identification

Real life power systems consist of thousands of buses. The high dimensionality of load parameter space presents considerable difficulties for the understanding of the loadability surface. In particular it is not easy to use a convenient graphical representation as in the 2-dimensional Figs. 1 and 2, from which it is easy to interpret loadability and design controls.

In this Section an attempt is made to obtain a meaningful 2-dimensional view, by grouping active loads into two components [3]. The first component denoted as P_A corresponds to the load consumed in the most affected part of the system, while the other one denoted as P_B is the load consumption in the remaining, relatively unaffected, part of the system.

$$P_A = \sum_{i \in A} p_i \tag{8a}$$

$$P_B = \sum_{i \in B} p_i \tag{8b}$$

In order to implement the above transformation we require a clear criterion for the distinction between groups A and B. To this purpose the information from normal vector calculated at the loadability limit is used. As seen in Fig. 1, the more dominant elements of the normal vector indicate the loads mostly responsible for the loadability limit. Based on the above observation, we propose an index for classifying the buses of a power system in the two groups defined above.

On the other hand for the proposed grouping to have a clear meaning geographical areas instead of individual buses are examined. This is achieved by calculating for each geographical area A_i an index F_i formed by the sum of all normal vector elements that correspond to active and reactive loads in the area:

$$F_i = \frac{1}{\dim(A_i)} \sum_{j \in A_i} n_j \tag{9}$$

The area indices are normalized so that the largest is equal to 1. Then we search for a clear split between the normalized values of indices, so that the areas with high indices form the affected region A, while the remaining ones form the relatively unaffected region B:

$$F_i\big|_{i \in A} >> F_i\big|_{i \in B}$$

3.4 Loadability surface visualization

Up to now we have described a method to calculate a loadability limit, as well as the smallest percentage of load increase to reach loadability subject to condition (3). Furthermore, the multi-dimensional vector of load powers was transformed to a 2-dimensional vector related to areas A and B defined above. Combining these results we can get a 2-dimensional image of the loadability surface as in Fig. 3, where the initial operating point, the uniform direction of stress and the loadability limit (black circle) along this direction are shown.

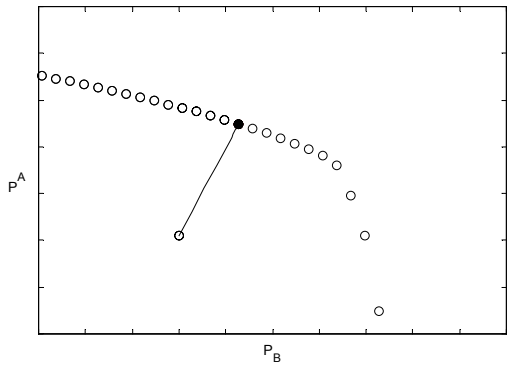

Figure 3: Loadability surface

In order to trace the other points on the loadability surface, we perform test simulation runs near the limit already found. This is done assuming equal percentages of load variation within each of the two regions A and B, c_A and c_B respectively:

$$\sum_{i \in A} \Delta P_i = c_A \sum_{i \in A} P_{io} = c_A P_{Ao} = \Delta P_A \tag{10a}$$

$$\sum_{i \in B} \Delta P_i = c_B \sum_{i \in B} P_{io} = c_B P_{Bo} = \Delta P_B \tag{10b}$$

where the coefficient ratio c_A/c_B defines the direction of variation in parameter space. Clearly the first loadability limit obtained is that for $c_A=c_B$. Note that a constant power factor is always assumed, so the above changes correspond to reactive loads as well.

For each new point in parameter space we attempt to solve the augmented system of equations (see section

3.2). If convergence to a stable long-term equilibrium is achieved, the load of the affected region is uniformly increased, until a new loadability limit is obtained. Otherwise, if the first attempted solution does not converge, loads of the affected region are uniformly reduced, and the procedure stops when the first solution point is found. This point will be the new loadability limit. In either case, each time a new loadability limit is found the procedure starts over again until a sufficient number of limit points is obtained.

When the above procedure starts, the new direction of load variation is arbitrarily chosen (e.g. horizontal by setting c_A=0). After that, the direction defined by the last two obtained limits is found to reduce the overall computational effort.

The set of all loadability limits thus obtained, forms a boundary of the feasibility region in the two-dimensional space of P_A and P_B, as shown in Fig. 3, provided that load variation within each area remains proportional.

4 APPLICATION TO THE HELLENIC SYSTEM

The snapshot of the Hellenic Interconnected system analysed here includes 892 buses, 526 transformers, 568 transmission lines, 101 generators and three external interconnections to the North of the country. The salient feature of the system is that the main production is located at the north (Western Macedonia), while the main consumption is in the metropolitan area of Athens. This leads to significant power transmission in the North-South direction.

At the initial operating point, the load of the system is 9084 MW. Exponential load model with exponents a=1.5 and b=2 is used to represent active and reactive power at all buses. The loads participating to the uniform load increase (7710 MW initially) belong to 8 geographical areas. The remaining load (P_C=1374 MW) corresponds to industrial loads and power plant auxiliaries and is assumed to remain constant during the simulation.

The method presented here was applied to the pre-contingency configuration, where the system was already highly stressed. As explained in section 3.2, a proportional load increase was imposed to assess the loadability margin of the system. In order to obtain accurate results the imposed rate of load ramp was reduced as the loadability limit was approached. The loadability limit corresponding to the uniform ramp was reached for a total consumption of 9480 MW. At this point the load participating in the ramp was 8107 MW. This corresponds to a loadability margin of 5.2% with respect to the initial operating point.

This loadability limit corresponds to an SNB. Therefore the left eigenvector **w** of the zero eigenvalue was determined providing through (1) the normal vector to the loadability surface. After checking that assumption (3) is valid, we calculate using (9) the index values for each of the 8 geographical areas. Absolute and normalized values of the index F_i are shown in descending order in Table 1. As seen, there is a clear separation between the areas, denoted by the heavy line at the middle of the Table. Indeed, the areas above the line have index values between 0.8 and 1.0, while the indices of other areas do not exceed 0.4. Based on this separation we perform the grouping of load buses into the affected area A and the remaining of the system B:

$$P_A = P_1 + P_2 + P_3 + P_4$$
$$P_B = P_5 + P_6 + P_7 + P_8$$

As expected, the affected areas include the metropolitan area of Athens and its neighbouring areas, while the relatively unaffected areas are located at the north and west of the country, close to the main generating stations. The most severe problems are experienced in Central Greece.

No.	Area	Index (F_i)	
1	Central Greece	0.61	1.00
2	Thessaly	0.54	0.89
3	Peloponnese	0.46	0.75
4	Athens metropolitan	0.42	0.69
5	Central Macedonia	0.25	0.41
6	Western Greece	0.24	0.40
7	North-eastern Greece	0.09	0.14
8	Western Macedonia	0.08	0.14

Table 1: Indices used for area identification

5 DETAILED QSS SIMULATION

5.1 Load Response

The above analysis to obtain the loadability limit and provide information on the loadability surface and margin sensitivity is based on the purposefully pessimistic assumption that all loads are restoring to their full power. As explained in Section 3, also the tap limits are ignored in this phase. These assumptions are trying to account for possible load recovery mechanisms within the distribution system that cannot be modelled using the data available at the control centre.

A different approach is used during the detailed QSS simulation, with which the effects of countermeasures, such as load shedding, are assessed. In this program the lower tap limits of the LTCs are explicitly enforced and load self-recovery is not considered. In this way the actual load increase achieved diverges from the demand that is still modelled as a uniform ramp. This is shown in Fig. 4, in the two dimensional load space defined above.

As seen in Fig. 4, the actual load increase follows at first the direction of the demand quite closely. However, because of LTC deadbands the actual load increase departs slightly from the uniform demand direction. As the system gets progressively more and more stressed, the LTCs in the affected region start to reach their lower tap limits and the load restoration process stops in this

area. Thus, the actual load increase in the affected region is much smaller than the increasing demand and the two curves (demand vs. consumption) differ considerably.

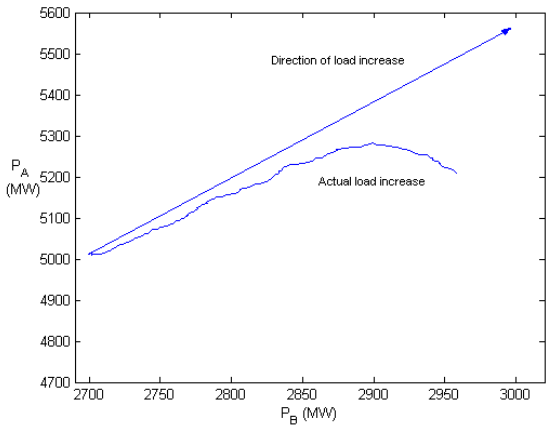

Figure 4: System evolution in the load power space

5.2 Stator current limits

Another significant factor modelled in the detailed QSS simulation and not present in the loadability limit computation program is the effect of stator current limit on synchronous generators.

In the Hellenic System there is no automatic limiter to adjust the stator current, thus the model adopted for the QSS simulation tries to imitate the suggested operator practice, in order to avoid stator overheating and the loss of the unit.

In general, the rotor current limit is taken to correspond to the rated generator output for rated voltage. Thus, for nominal voltage the rotor current limit is more restrictive at all load levels below the rated active power. However, turbine efficiency improvement [10], or continuous decrease in the generator terminal voltage during a voltage instability scenario, may lead to excessive armature current, thus making armature limit more restrictive than the field limit.

Automatic armature current limiters are common only in few countries, e.g. Sweden [11]. Usually these limiters operate by lowering generator reactive production. In this case the limiter acts directly on the excitation system producing a signal, which is subtracted from the main summing junction of the AVR. In some cases the generator active power production can also be reduced.

In the QSS simulation program used here the armature current limitation is affected first by ramping down the active generator power. Thus, if the stator limit violation remains for more than a specified time delay (e.g. 20 s) the active generation is reduced at a specified rate until either the violation is removed, or the technical minimum of the unit is reached.

If the stator overload remains after reaching the technical minimum, current limitation is obtained by decreasing the reactive power. This is implemented through an adequate decrease ΔV of AVR voltage reference. If the generator is operating under AVR control, the reference voltage decrease rate is constant. If the machine is operating under field current limit, an adequate step ΔV is calculated, so that the generator switches again to AVR operation. After this point, the reference voltage decrease continues for as long as the armature current violation persists. The results of applying armature current limitation to two generators of the Hellenic System are shown in Fig. 5, where the armature current as a function of time is plotted for a load-shedding scenario.

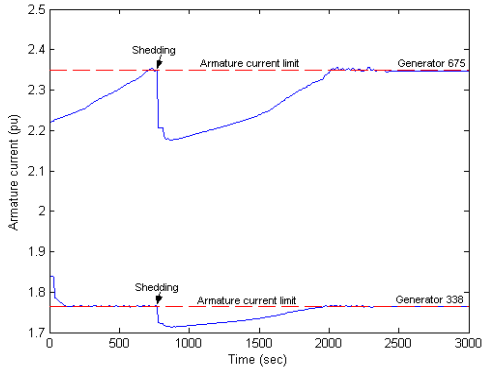

Figure 5: Armature current limitation

6 APPLICATION OF LOAD SHEDDING

6.1 Load shedding scheme

Load shedding is in many cases the ultimate countermeasure to restore a long-term equilibrium during emergency conditions. Reactive element switching and generator rescheduling have no impact on consumers and should be normally the first to be utilized if available. LTC controls, such as tap-blocking, tap-reversing, tap-locking and distribution voltage setpoint reduction, assume voltage sensitive loads and do not restore a long-term equilibrium in the presence of load self restoration [12].

In this Section we consider the problem of insufficient loadability margin, when the projected load increase is larger than the loadability limit computed as in Section 3. To overcome this emergency situation an amount of load has to be shed, in order to allow the system to survive the expected demand. Thus a known amount of margin increase $\Delta\mu$ is required.

The load-shedding scheme proposed here assumes a constant shedding fraction s at each load bus. To determine the amount and location of load shedding the sensitivities of the margin $S_{\mu Pi}$ calculated from (6) are used and buses are ranked according to decreasing sensitivities. The achieved increase in loadability margin is:

$$\Delta\mu = \sum_{i=1}^{n} S_{\mu P_i} \Delta p_i \qquad (11)$$

where:

$$\Delta p_i = -sP_{oi} \qquad (12)$$

is the amount of load shed at bus i. Note that sensitivities are negative, thus the margin increases when shedding load.

Load is shed first at the most sensitive bus and the shedding continues until the desired margin increase is achieved. The procedure is similar to [4] and guarantees the minimum amount of shedding (in MW) for the specified margin increase. Note that the above procedure gives both the amount ("*how much*?") and the location ("*where*?") of load shedding. The time question ("*when?*") is not addressed here.

The buses selected for load shedding normally belong to the most affected area, since the largest sensitivities correspond to buses located in this area.

6.2 Application to the Hellenic System snapshot

The above load shedding scheme is applied to the snapshot of the Hellenic system presented in Section 4. As mentioned in this Section, the calculated loadability margin for this system is 396 MW for uniform load increase, or 5.2 % of the load participating in the ramp. In order to test load shedding, a demand increase of 11% is assumed. Thus we require a margin increase of 5.8%, or 447 MW. Applying equation (11) with a load shedding percentage s=0.15 we end up shedding load from 69 buses. The total load shed ΔP is 260 MW (sensitivities in MW are larger than 1, varying from -3.5 to -1.4 in the buses where shedding is applied) and is distributed among the four affected regions as shown in Table 2.

Area	Load shed (MW)
Athens metropolitan	108
Central Greece	81
Peloponnese	48
Thessaly	23
Total ΔP	**260**

Table 2: Load demand shedding in each area

Load restoration in the P_A, P_B plane discussed in Section 3 is shown in Fig. 6 with and without load shedding. Point L is the loadability limit before load shedding.

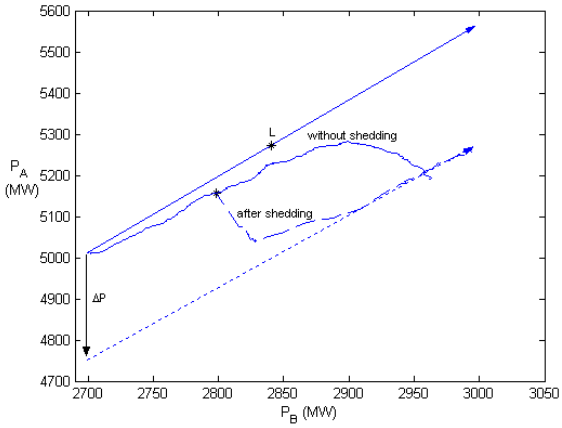

Figure 6: System evolution in the load power space

Without load shedding the system cannot sustain the 11% ramp and load in the affected area drops significantly due to tap limits. After load shedding the remaining load demand is met successfully.

The same can be seen in Fig. 7, where the voltage response at a critical bus is shown without load shedding and for shedding corresponding to different levels of $\Delta\mu$. The trajectory shown with solid line corresponds to an increase in loadability margin $\Delta\mu$=444 MW. This leads to an acceptable voltage level at the critical bus after shedding. In contrary, for $\Delta\mu$=398 MW (corresponding to the dashed line) and $\Delta\mu$=348 MW (corresponding to the dotted line) an unacceptable voltage level at the bus. Thus, without load shedding the voltage is practically collapsing, while for a smaller amount of shedding the voltage is not satisfactory.

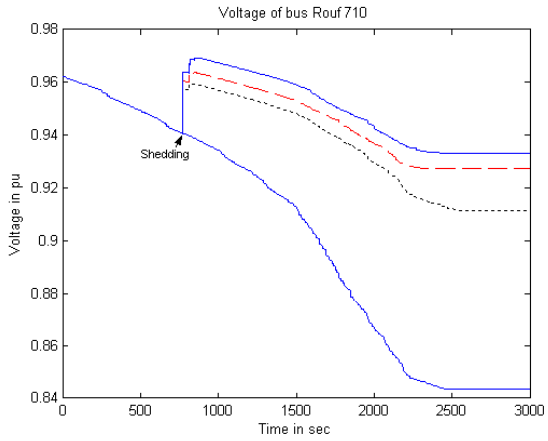

Figure 7: Voltage evolution for various shedding actions

7 CONCLUSIONS

In this paper we presented a unified approach for loadability limit determination, analysis of voltage instability and design of load shedding during emergency situations.

At first a technique to obtain a loadability limit is presented based upon a uniform load ramp. Under the condition that all loads contribute to the loadability, this limit provides the smallest percentage of load increase that can cause instability. This percentage can be easily translated also to a MW value.

The information obtained from the normal vector to the loadability surface were used to identify which areas belong to the affected region of the systems, following which a two-dimensional load space was defined where the loadability surface, as well as the load evolution during a simulated disturbance can be visualized. This allows an easy interpretation of loadability limits that could facilitate the understanding of control centre operators.

During emergency situations, when the expected load increase exceeds the available loadability margin, a load-shedding scheme was designed based on margin sensitivity to restore a stable and secure operating point of the system. The load shedding performance is validated using a QSS simulation program, which includes

also a model for armature current limitation of generators using active and reactive power control.

All the techniques presented in the paper were applied to a heavily stressed snapshot of the Greek system taken shortly before the blackout of July 12.

REFERENCES

[1] T. Van Cutsem, C. Vournas, "Voltage Stability of Electric Power Systems", Kluwer Academic Publishers, 1998.

[2] C.D. Vournas, N.G. Maratos, M. E. Karystianos "Exploring Power System Loadability Surface with Optimization Methods", Bulk Power System Dynamics and Control V, Onomichi, Japan, Aug 26-31, 2001.

[3] T. Van Cutsem, J. Kabouris, G. Christoforidis, C. D. Vournas "Application of Real-Time Voltage Security Assessment to the Hellenic Interconnected System", IEE Proc. GTD, 152:123-131, Jan. 2005.

[4] C. Moors, T. Van Cutsem, "Determination of optimal load shedding against voltage instability", 13th PSCC, Trondheim, June 1998, pp. 993-1000.

[5] S. Greene, I. Dobson, F. Alvarado, "Sensitivity of the loading margin to voltage collapse with respect to arbitrary parameters", IEEE Trans. on PWRS, 12:262-272, 1997.

[6] I.A. Hiskens, R.J. Davy, "Exploring the Power Flow Solution Space Boundary", IEEE Trans. on PWRS, 16:389-395, 2001.

[7] C. Vournas, M. Karystianos, "Load tap changers in emergency and preventive voltage stability control", IEEE Trans. on PWRS, 19: 492 - 498, Feb. 2004.

[8] I. Dobson, L. Lu, "Voltage collapse precipitated by the immediate change in stability when generator reactive power limits are encountered", IEEE Trans. on Circuits and Systems Part I: Fundamental Theory and Applications, 39: 762-766, Sept. 1992.

[9] F. Alvarado, I. Dobson, T. Hu, "Computation of Closest Bifurcation in Power Systems", IEEE Trans. on PWRS, 9:918-924, 1994.

[10] S. G. Johansson, D. Popovic, D. J. Hill and J. E. Daalder, "Avoiding Voltage Collapse by fast Active Power Rescheduling", Int. Journ. of Elec. Power and Energy Systems, 19:501-509, 1997.

[11]S. G. Johansson, F. G. Sjogren, D. Karlsson and J. E. Daalder, "Voltage stability studies with PSS/E", Bulk Power Systems Dynamics and Control III, Davos, Sep. 1994, pp. 651-661.

[12]C. D. Vournas, A. Metsiou, M. Kotlida, V. Nikolaidis, M. Karystianos, "Comparison and Combination of Emergency Control Methods for Voltage Stability", IEEE/PES General Meeting, Denver, 2004.